Uni-RXN: A Unified Framework Bridging the Gap between Chemical Reaction Pretraining and Conditional Molecule Generation

Bo Qiang¹, Yiran Zhou¹, Yuheng Ding¹, Ningfeng Liu¹, Liangren Zhang¹ and Zhenming Liu^{1*}

^{1*}State Key Laboratory of Natural and Biomimetic Drugs, School of Pharmaceutical Sciences, Peking University, Beijing, 100191, China.

*Corresponding author(s). E-mail(s): zmliu@bjmu.edu.cn; Contributing authors: bqiang@bjmu.edu.com; yrzhou@bjmu.edu.cn; yh_ding@bjmu.edu.cn; liuningfengdede@pku.edu.cn; liangren@bjmu.edu.cn;

Abstract

Chemical reactions are the fundamental building blocks of drug design and organic chemistry research. Machine learning for chemistry is a rapidly advancing field with numerous applications. In recent years, there has been a growing need for a large-scale deep-learning framework that can efficiently capture the basic rules of chemical reactions. In this paper, we have proposed a unified framework that addresses both the reaction representation learning and molecule generation tasks, which allows for a more holistic approach. Inspired by the organic chemistry mechanism, we develop a novel pretraining framework that enables us to incorporate inductive biases into the model. Our framework achieves state-of-the-art results on challenging downstream tasks. By possessing chemical knowledge, this framework can be applied to reaction-based generative models, overcoming the limitations of current molecule generation models that rely on a small number of reaction templates. In the extensive experiments, our model generates synthesizable drug-like structures of high quality. Overall, our work presents a significant step toward a large-scale deep-learning framework for a variety of reaction-based applications.

Keywords: Chemical Reaction, Large-scale Pretraining, Molecule Generation

1 Main

Deep learning models have revolutionized many fields of researches [1–3]. In particular, deep generative models [4, 5] and pretraining models [6] have shown promise in drug design. Machine-learning models need to be built for specific tasks which require a time-consuming from-scratch training process. With the rapid development of large-scale pretraining models [7, 8], machine-learning models can be built for small datasets via efficient finetuning.

Chemical reactions are the foundation of drug design and organic chemistry studies. Currently, data-mining works have enabled deep learning models to be applied to chemical reactions. USTPO[9, 10] is the current largest opensource database developed by Lowe through text mining. Based on these data, there have been plenty of data-driven works that intend to delve into the representation learning on chemical reactions. Representation learning refers to the process of automatically learning useful features or representations of data, which can then be used for various downstream tasks such as classification or clustering [11]. In earlier works, traditional molecular fingerprints were applied directly for reaction representations[12, 13]. Inspired by natural language processing (NLP) methods and computer vision (CV) methods, researchers also applied attention-based network[14] or contrastive learning techniques[15, 16] in chemical reaction pretraining networks. These representations have been tested on classification tasks[17] or regression tasks[18]. However, these methods ignore the fundamental theories in organic chemistry, which limits their performance. For example, every atom or bond outside the reactive centers can be masked to mimic the masking from SimCLR[19] in RxnRep[15]. However, electronic effects and inductive effects which play important roles by changing the electron density within a few bond distances would be neglected if the reactive centers are exclusively considered.

Except for reaction classification tasks, molecule generation based on chemical reactions is also an important application. This branch of models has been proven to be capable of generating synthetically accessible molecules. [20–23]. Earlier works always applied a step-wise template-based molecule generation strategy. At each step, a fragment building block and a reaction template are chosen to concatenate with the existing structures. These template-based methods highly depend on predefined building blocks and reactions, which narrow down the accessible chemical space. Similar trends are found in the field of reaction product prediction, in which template-based methods[24] cannot be extrapolated to complex reactions, and this problem is solved by using template-free methods [25, 26]. In the reaction-based molecule generation task, template-free methods [27, 28] have also demonstrated advantages in generalization over templated-based methods. Nevertheless, these methods were only designed for de novo molecule generation. In other words, they are unable to generate molecules based on the given molecules. Therefore, there is an urgent need to develop a novel structure-conditional generative model in a template-free manner.

In this paper, we propose a novel unified deep learning framework for chemical reactions, which can be applied to the self-supervised representation learning and conditional generative model. Instead of using mask prediction tasks or contrastive learning, we have designed a series of well-defined self-supervised tasks which are particularly for chemical reactions, including active center prediction, main-reactant sub-reactant pairing tasks, and reactants products pairing tasks. Our method has achieved state-of-the-art results on challenging reaction classification tasks. The results have indicated that the model could efficiently capture the domain knowledge of chemical reactions, which enables a variety of downstream applications.

Since our model captures chemical rules efficiently, it can be applied to the generative task. Instead of choosing fragments from a predefined reactants library, our model takes molecular structures as input conditions and outputs the representations of the corresponding reactants while maintaining permutation invariance. With the help of the dense vector similarity searching package, reactants can be retrieved from any user-specified reactants set efficiently. At last, a pluggable reaction prediction model is utilized to predict the products as the output results. Compared to template-based methods that explore a limited subset of the chemical space, our method generates more synthetically accessible drug-like structures and is more suitable for virtual library enumeration, which is demonstrated by the case studies and statistical results.

2 Related Work

In this section, we discussed two related branches of related works, chemical reaction pretraining and reaction-based molecule generation.

There has been plenty of works that address the task of representing the chemical reaction. The differences between traditional molecule fingerprints, for example, Morgan Fingerprint and Atom Pair Fingerprint of reactants and products are utilized to represent the subgraph changes in chemical reactions [12]. Later, based on the hypothesis that chemical reaction is the rearrangement of different functional groups, rule-based representations [13] are developed, and they can be applied to the classification of reactions. To further improve the performance on some harder downstream tasks, the deep learning based representations are proposed. Rxnfp [14] is the first pretraining framework on reactions in which a BERT-like [1] mask language learning method is applied directly to build models on chemical reaction smiles sequence from a commercial reaction database. With the help of large-scale hand-curated data, the model achieves impressive outcomes. However, the graph is a more informative representation than the smiles texts. Therefore, a few research [15, 16] adapted graph neural networks to chemical reactions using contrastive learning. In our methods, we apply multimodal representations for reactants and reagents and trained both graph-based and text-based transformers to derive the representation of chemical reactions.

In addition to pretraining networks, the molecule generative model based on chemical reactions is also an important application of deep learning in the chemical reaction space. Generative models aim to sample similar but different data points from the original data distribution, which can be applied to develop large-scale drug-like molecule vocabulary. In order to make the generated structure accessible, the chemical reactions-based method is designed to generate molecules with desired properties [20, 27, 28]. For example, ChemBO [20] applied Bayesian optimization in the latent space to find the desirable molecules. However, in most cases which property is directly related to drug likeness is unclear. Hence, models [21–23] have been proposed to generate analogues based on the input target structure for ligand-based drug design. For example, C-RSVAE [23] is developed to generate synthetic routes for molecule generation using reaction templates and fragment building blocks, which generate large numbers of molecules with desirable properties. However, because of the limited power of template reactions, these models can only generate molecules from scratch with predefined reactions. To solve the above problems, we propose our generative framework that is able to directly generate novel molecules similar to the seed molecule in a template-free fashion.

Results and Disscusion

3.1 Challenges in Chemical Reaction Modeling

There are several ways to convert chemical reactions into machine-readable structural data. We define the chemical reactions in the following form to include most of the raw data:

$${\{\operatorname{Reactant}_{i}\}, i \in m \xrightarrow{\{\operatorname{Reagent}_{j}\}, j \in n} \operatorname{Product}}$$
 (1)

Chemical reactions involve three main components: reactants, reagents, and products. Reactants are structures that contribute certain substructures to form the products, and the reactant whose atoms are maximally matched with the product is defined as the main reactant. Other reactants are denoted as sub-reactants. Reagents are chemical entities that do not map to any atoms in the product structures but are necessary for providing certain chemical conditions, such as solvents or acids. To jointly model the probability of reactants, reagents, and products, there are three main challenges. Firstly, complicated organic chemical propositions such as electron rearrangement indicate the dependency within the reactants and reagents, which is too hard to model when the mechanisms are not provided in the public dataset. Intuitively, when the sub-reactants or reagents are altered, the chemical reactions are most likely to fail. Secondly, the reactants and reagents are permutation invariant, which means that when we change the input order of the reactants or reagents, the product will be constant, hence simply applying order deterministic mask language model [14] is not suitable for this problem. The final challenge is that

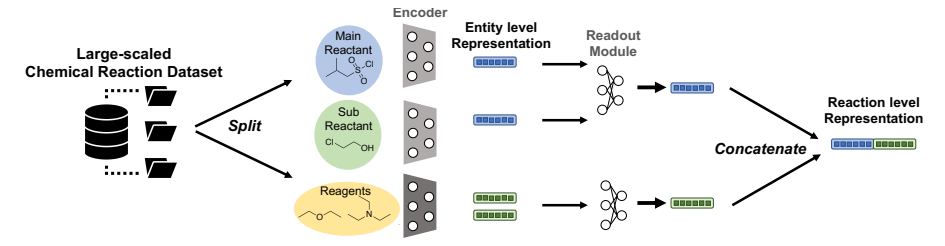


Fig. 1 An overview of the unified framework of Uni-RXN. The atom mapping is utilized for splitting the reactants into the main reactant and sub-reactants. Then, a multimodal graph/text-based transformer model is applied for deriving the chemical entity-level representations. Entity-level representations are further fused into reaction-level representations.

reagents and reactants play different roles in chemical reactions, which makes the modeling challenging.

In order to address the above challenges, we design a novel unified framework for modeling chemical reactions. The first challenge comes from the reaction's complicated underlying mechanism is solved by contrastive learning and reactive center prediction task, which will be discussed in detail in Sec. 3.2.1. The second equivariant challenge is solved by shared parameters in encoding as in Fig. 1 and a permutation invariant generative network in decoding. The last challenge is solved by applying a multimodal network for reactants and reagents, which extract information in different manners. Specifically, a graph-based transformer is applied to process reactants and products, and a text-based transformer is applied to process reagents. We will discuss the pretraining and generative models respectively in Sec. 5

3.2 Pretraining Framework and Downstream Tasks

3.2.1 Self-supervised Contrastive Learning

The key components of contrastive learning are the methods of negative data sampling. Rather than dropping or masking atoms outside the reactive center, which would result in a loss of information, we adopt a different strategy illustrated in Fig. 2 a. Our model tends to encode two fundamental aspects of chemical reactions.

Firstly, we model the interactivity between the main reactant and the combination of sub-reactant and reagents (denoted as 2-tuples sub-reactants, reagents below). It is well-recognized that the dataset of the chemical reactions is biased. Specifically, only optimized and widely used chemical reactions are curated in the public patent datasets. Therefore, the model only trained on the public dataset will fail to capture any information of negative data (i.e., invalid reactions). To address this, we apply the contrastive loss on reactants and reagents where the negative samples are generated by the random permutation of sub-reactants and reagents among the positive reactions (See Sec. 5). We use Information Noise-Contrastive Estimation (infoNCE) as the training objective, projecting the embeddings of the main reactant and {sub-reactants,

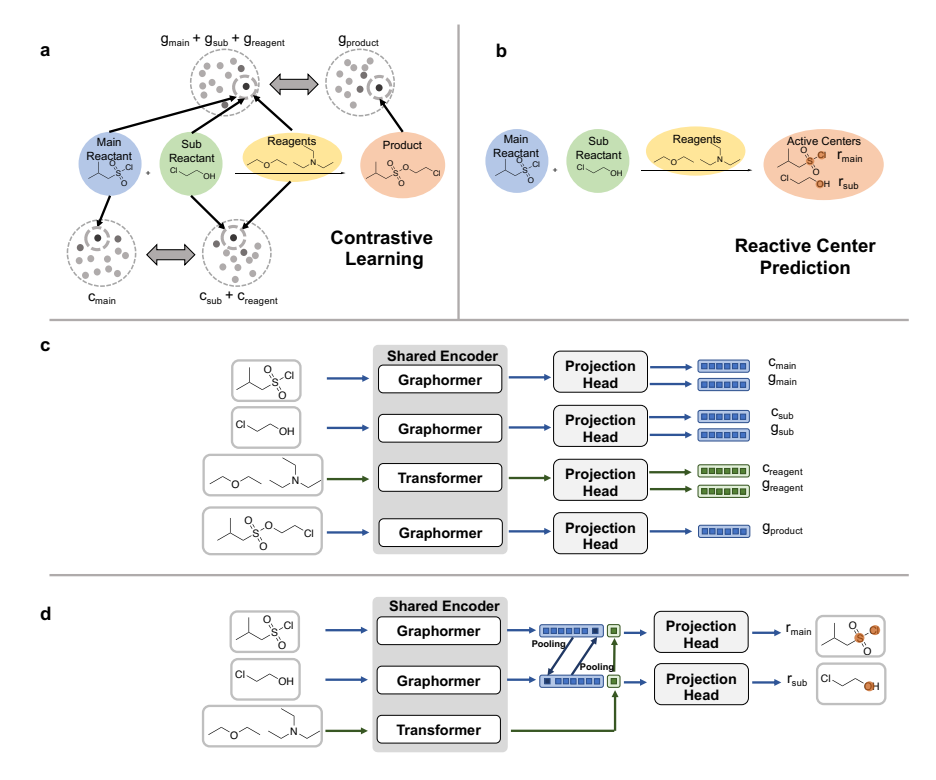


Fig. 2 (a) Two contrastive learning tasks we utilized for pretraining. The main reactant, sub-reactants, and reagents are projected into the embedding space using different attention-based model architectures. The similarity between the embeddings of {main reactant} and {sub reactants, reagents} is maximized because of the underlying organic mechanism. The similarity between the embeddings of {main reactant, sub reactants, reagents} and {product} is maximized because of the graph-level mapping. (b) An illustration of the reactive center prediction task. (c) The model architecture for contrastive learning. c stands for the chemical training signal which is applied in the first contrastive learning objective. While g stands for the graph training signal which is applied in the second contrastive learning objective.. (d) The model architecture for reactive center prediction tasks. An additional graph-based transformer model is applied to identify the place where chemical bonds are broken or newly formed in chemical reactions.

reagents} into the same embedding space with different MLP projection models. When there are multiple sub-reactants or reagents a read-out module is applied. This approach maximizes the similarity between paired main reactants and {sub-reactants, reagents} in the embedding space. The training objective is inspired by the powerful generative pretraining model GPT-2/3 [29] where the main reactant and sub-reactants, reagents in our model mimic its context and next time-step token, respectively, which enables us to develop the conditional generative model that is discussed in detail in Sec. 3.3.

Secondly, we seek to model the functional group rearrangement and structure transformation between the combination of main reactant, sub-reactants, and reagents (denoted as 3-tuples main reactant, sub-reactants, reagents) and

product. Under the chemical condition provided by the reagents, the functional group within the main reactant and sub-reactants are rearranged. In order to learn this transformation process, based on the same encoder, we apply another set of projection heads to predict the embeddings of {main reactant, sub reactants, reagents} and product. A similar training process is performed as the first contrastive learning task, in which the paired similarity between {main reactant, sub-reactants, reagents} and product in the embedding space is maximized.

By leveraging these two fundamental aspects of chemical reactions, our contrastive learning framework is able to learn from biased and unoptimized data and generate rich representations.

3.2.2 Reactive Center Predition

Aside from contrastive learning, our model is also trained to predict the reactive centers in chemical reactions as in Fig. 2b. In our work, we define atoms as chemical reactive centers if they undergo chemical state change. The chemical state is defined as the formal charge, the hybridization, and the neighbor atom types of a certain atom. We propose to use another graph-based transformer model instead of MLP as the projection head, which will be discussed in detail in Section 5. This pretraining task further helps our model to understand the position effect in chemical reactions, which is always ignored in related works.

Table 1	The accuracy of	the chemical	reaction	classification

Reaction Number per Class	Rxnrep	MolR	DRFP	Uni-RXN
4 8 16 32 64 128	0.169 ± 0.0227 0.225 ± 0.0080 0.305 ± 0.0106 0.375 ± 0.0159 0.439 ± 0.0078 0.489 ± 0.0036	$\begin{array}{c} 0.249 \pm 0.0165 \\ 0.328 \pm 0.0173 \\ 0.429 \pm 0.0213 \\ 0.526 \pm 0.0076 \\ 0.615 \pm 0.0022 \\ 0.692 \pm 0.0025 \end{array}$	0.258 ± 0.0382 0.343 ± 0.0159 0.424 ± 0.0108 0.498 ± 0.0059 0.559 ± 0.0044 0.617 ± 0.0059	$0.570 \pm 0.0152 \ 0.660 \pm 0.0128 \ 0.739 \pm 0.0116 \ 0.781 \pm 0.0080 \ 0.824 \pm 0.0040 \ 0.850 \pm 0.0028$

The accuracy is computed multiple times on different random samples. The Standard Deviation(std) of the accuracy is listed after \pm . The higher accuracy indicates better performance. Trained graph neural network encoder from Rxnrep, MolR is applied to compute the baseline model representation. The package that computes DRFP representation is downloaded directly from rxn4chemistry

3.2.3 Reaction Classification

After completing the two pretraining tasks on the USTPO MIT dataset, we use the shared encoder to generate representations for downstream tasks. To ensure a fair comparison, we do not split the main reactants and sub-reactants when generating representations. Most previous works evaluated their representation on TPL 1k dataset for reaction classification and reach over 90

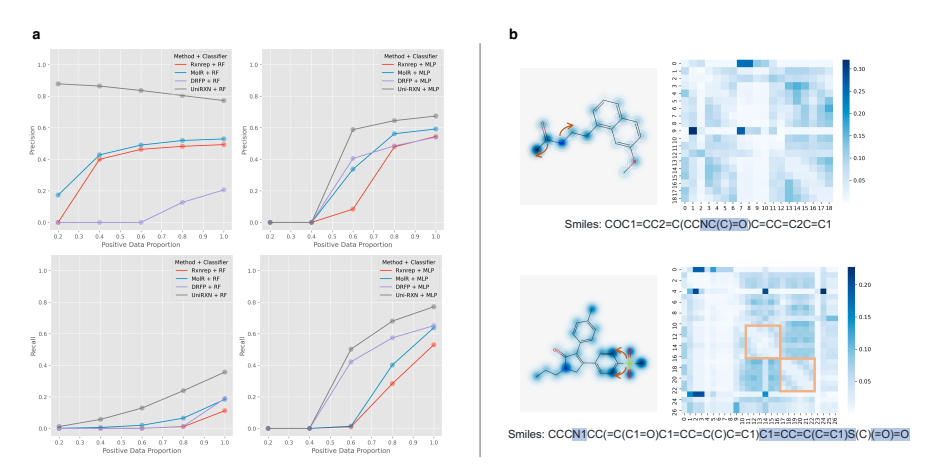


Fig. 3 (a) The line chart illustrates the precision and recall of different representations in the chemical reaction error identification task, the horizontal axis denotes the ratio of the number of positive data to the number of negative data. (b) The attention map of the graph-based transformer encoder. The darker color means a higher self-attention score. The atoms with high attention scores are also highlighted in the smiles sequence.

percent accuracy. Our model provides comparable performance on this dataset, which the results are provided in the Supplement Information. We also choose a more challenging reaction classification dataset, Schneider [12], which used a comprehensive oncology system. When generating the representation, we mask the product of the chemical reactions to prevent the model from relying on simple graph pattern recognition. To make the classification even harder, we unbias the dataset by randomly drawing the same number of reactions for each class both in the training and testing dataset, following previous work [15]. The results on this balanced benchmark dataset are demonstrated in Tab 1.

Logistic Regression (LR) Classification offered by the cuML package is applied here as the reaction classification heads based on the chemical reaction representations. We denote our representation as Uni-RXN and compared it with three baseline models that are able to derive representations when the product structure is masked. The accuracy of predicting the correct reaction class drastically decreases when the number of reactions per class drops from 128 to 4. In the range of dataset sizes we tested, our model has outperformed the baseline models by a large margin, especially on small training sets. Our model predicts more than half of the reaction classes with only 4 reactions per class for training. Notably, we keep the encoder parameter fixed when comparing our model with other baselines. Our model demonstrates impressive results without finetuning any parameters. In conclusion, Uni-RXN is a powerful tool to classify chemical reactions even without product information which shows great potential in reaction forward prediction applications.

3.2.4 Reaction Error Detection

Another downstream important task is error detection in chemical reactions. The main challenge in molecule generation based on template-free chemical reactions is the extrapolation ability. The generator needs to avoid generating unsuccessful chemical reactions despite having only successful reactions available for training. Additionally, in reaction optimization tasks, the limited number of negative data hinders the usage of machine learning models to search for the correct reagents or sub-reactants. Therefore, we evaluate the ability of our pre-trained encoders to identify unsuitable sub-reactants and reagents. To this end, we constructed a dataset that includes both positive, successful chemical reactions and negative, noisy chemical reactions as discussed in Sec. 5. We test Uni-RXN's ability to differentiate between them. As illustrated in Fig. 3a, our model outperforms other baseline models in all cases. In real scenarios, the proportion of negative samples varied in different kinds of reactions, so experiments with different numbers of positive data are carried out. The results show that when the positive/negative ratio is 0.2, every representation failed to recall any positive data from the test set. However, with the proportion of positive reactions increasing, our method gradually shows a higher recall rate than the baseline methods. The precision metric shows similar trends. In conclusion, our representation can be applied to reaction error detection tasks when extremely low positive data is available and improves the performance of machine learning models on chemical reaction optimizations. This also shows that existing representations have learned from the undesirable data bias.

3.2.5 Visualization of Attention

The visualization of the Transformer attention reveals how the model processes the input graph. We visualize the attention weight in Fig. 3b. The attention maps show that our model learns to focus on the reactive part of the input main reactant molecules. Heteroatoms that are active in chemical reactions have higher attention scores compared to carbon chains. Besides this simple proposition that is easy to learn by models, more complicated rules involve the interaction between neighbor functional groups that are also encoded. For example, when there is a strong electron-withdrawing group on the benzene ring, the ortho-position becomes more reactive. Our encoder clearly captures this basic chemical rule and learns to focus on the ortho-position. The attention maps are also well-clustered. The self-attentions between atoms in the same aromatic ring are low because of their shared electron cloud. These atoms have similar embeddings within the graph-based transformer model. However, the attention between neighbored functional groups is highly scored since their relations define the behavior of the reactants in organic chemical reactions.

3.3 Conditional Generation Framework and Drug-like library design

In addition to its effectiveness in classification tasks, our model also shows great promise in structure conditional generation tasks. In traditional medicinal chemistry research, hundreds of analogues are often synthesized from a hit structure to study the Structure-Activity Relationship (SAR). To simplify this process, we propose a generative model based on our pre-trained encoder that can derive as many synthesizable analogues as possible from a known structure. However, generating analogues through chemical reactions on a seed structure poses a challenge. In template-based methods, if we denote the number of reaction templates as T and the number of building blocks as B, the upper limit of the sampling space size is T*B. This space is so sparse that for some of the molecule inputs the space size is reduced to \emptyset , which is shown by experimental results in Sec. 3.3.1.

To overcome this challenge, we develop an auto-regressive generative model that efficiently generates the corresponding sub-reactants and reagents for a given input molecular structure within a constrained infinite subspace. Our path-aware network defines a sequence of chemical reactions, in which the product of the former reaction is the input main reactant of the latter reaction. During the molecule-generating process, our model operates like a chatbot with rich chemical knowledge. The user simply queries the model about which reaction can be applied to the existing structure, and our model outputs the response structures that include sub-reactants and reagents iteratively, as illustrated in Fig. 4a. At the modeling level, our model first generates the representation of the full response structures using variational inferencing and then generates the individual representation using a set generator as in Fig. 4b. The set generator is designed to decode all representations permutation invariantly. During the training phase, the generated representation is trained to approximate the representation from the ones encoded by our pretrained encoder. In the generation procedure, the generated representation is used to retrieve reactants and reagents from a user-specified large commercially accessible molecule library. We use the reactive fragment-like subset of ZINC [30] as our sub-reactants library, which contains 1 million structures. For the reagents library, we collect all reagents from the USTPO_STEREO dataset [31]. Once the model generates responses, another network predicts the product of the proposed new reactions. Our model provides an efficient and effective workflow for generating chemical analogues. More implementation details can be found in Sec. 5.1.2. To assess the accuracy and quality of the generated reactions, we provide an additional experiment with a module that predicts the reaction yield in Supplement Information B.3. Also, we observe that the target representations can be found at the top 12.43% similar representations in the library, indicating our model generates representations accurately. We will discuss the quality of the generated molecules in the following sections.

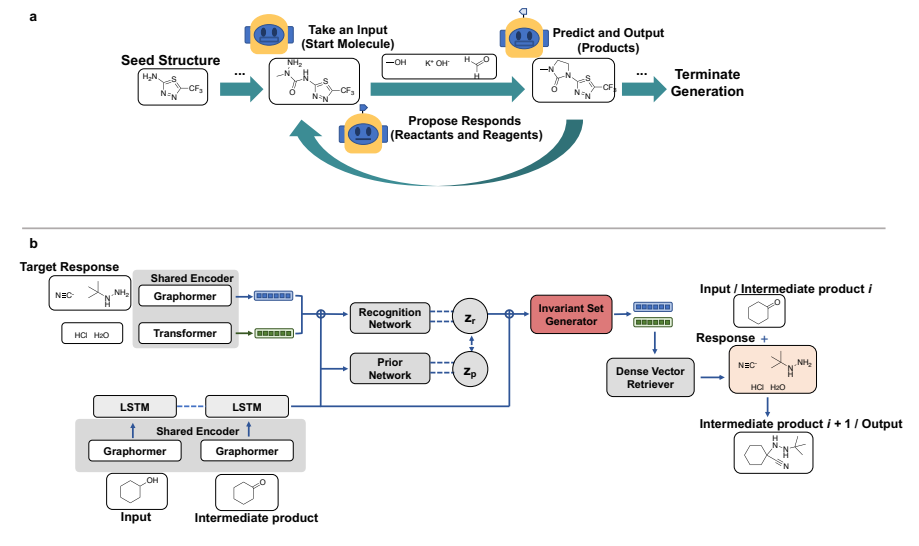


Fig. 4 (a) An overview of the generation framework. A sequential process is proposed to generate the analogues. At each step, the model proposed the sub-reactants and reagents, then the reaction predictor outputs the product. The product is fed to the model as the input for the next step until the termination criterion is met.(b) The model architecture of the generative model. The pre-trained model is utilized here as the encoder for target structures and main reactant inputs.

To evaluate our model's capacity of generating similar molecule structures conditioned on the input seed molecules, we use 2256 structures from the Drugbank database [32] to derive large drug-like datasets using our generative model. We compared our model with three baseline methods. SynNet (Denovo) and DINGOS (Denovo) are models that take the seed molecule's fingerprint as input and generate analogues by using template reactions from scratch. DINGOS (condition) is the method that specifies the seed molecules as starting molecules and then generates analogues by matching template transformations on them. These chemical reaction-based baselines are also tested to generate analogues conditioned on the drug structures.

3.3.1 Properties Evaluation

In order to evaluate the generated structures, we computed several basic drug-like properties and compared them with the real drugs, as shown in Fig. 5a. We aim to generate molecules with a close property data distribution to real drugs. It is evident that the DINGOS(condition) model generates molecules with a shifted chemical property distribution despite performing only a few steps of reaction modification on the seed molecules. Our model have outperformed template-based methods on the metrics of QED and molecule weight, generating a virtual library with the closest distribution compared

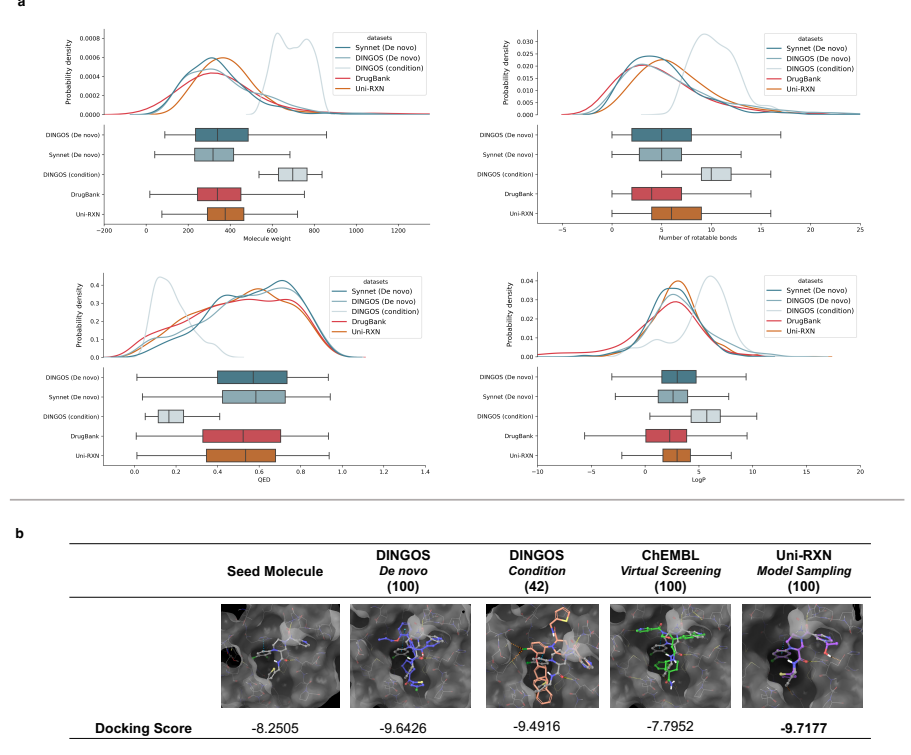


Fig. 5 (a) The properties of the drug-like molecule generated by different reaction-based molecular generation models. (b) The docking pose of the top scoring generated COVID-19 3CLPro inhibitors, the gray poses are the reference poses of the seed molecule derived from the original PDB file. The scaffold of the Uni-RXN generated molecule aligned perfectly with the reference pose.

to the seed molecules. Although all models generated molecules with more lipophilic structures, our model and SynNet still produce molecules with logP scores within the box range of DrugBank. Additionally, all generative models generate molecules with more rotatable bonds, which expands the 3D conformation space and offers assistance in discovering new analogues.

This paper goes beyond assessing the drug-likeness of molecules generated by our Uni-RXN model, as we also use synthetic accessibility scores to evaluate their synthesizability. To accomplish this, we apply three different metrics (SAScore [33], SCScore [34], and RA [35]), and the results are presented in Tab. 2. Among all the methods, only our model and DINGOS(condition) are able to generate molecules directly from the input structure, other methods need more reaction steps to generate from scratch. Unlike DINGOS(condition), which generates larger molecules due to the lack of decomposition reaction in the predefined templates, our generated molecules scored favorably on the SAScore and RA metrics, indicating that they are easier to synthesize than the input seed molecules. However, the SCScore provides the opposite results.

This is reasonable given that our generated molecules are derived by directly modifying the seed molecules via 1-3 chemical reactions, and the hypothesis behind SCScore is that the product is always harder to synthesize than the reactants in chemical reactions. Template-based de novo methods generate molecules distance to the seed molecules and have obvious distribution shifts on SAScore and RA. In combination with the distance metrics, it could be observed that DINGOS (De novo) and SynNet (De novo) sacrifice drug similarity and validity for lower synthetic accessibility scores, respectively. It indicates that the template-based methods tend to generate excessively simple molecules, which is undesirable in drug discovery research. Furthermore, our proposed modifications require fewer reaction steps to perform than to carry out a from-scratch complicated route by multiple template reactions. Overall, our approach provides a more effective way to generate molecules based on available drugs, where (1) fewer steps of chemical reactions are required and (2) the generated molecules exhibit a decent balance between drug similarity and synthetic accessibility.

Table 2 Evaluation of Synthetic Accessibility Scores, Validity, Chemical Distance and Scaffold Diversity

	SAScore ↓	SCScore ↓	RA ↑	Valid(%)	Chemical Distance	Scaffold Diversity
Seed Molecules	3.627	3.078	0.703	_	_	5.881
SynNet (De novo)	3.026	3.114	0.830	66.61	0.5131	5.774
DINGOS (De novo)	2.919	2.879	0.848	100.00	0.6283	5.809
DINGOS (condition)	3.845	4.937	0.636	45.81	0.8236	5.601
Uni-RXN	3.284	3.454	0.725	100.00	0.5041	6.603

 \downarrow indicates that the lower score means the molecules are easier to synthesize, while \uparrow indicates that the higher score means the molecules are easier to synthesize. A lower chemical distance means the generated molecules are more similar to the input structures, and a high chemical distance means the generated molecules failed to mimic the target structure. The scaffold diversity is measured by information entropy, and a higher value means fewer dominant scaffolds in the generated data.

Validity is also an important metric because an ideal model can generate analogues and modify valid structures as many as possible, based on the seed molecules. However, SynNet and DINGOS (condition) though generates synthesizable molecules, can only generate analogues for a limited proportion of input molecules. As for the DINGOS (*De novo*), though it achieved an 100% validity, its usage of template reactions and building blocks hinders its generalization to downstream applications. At last, we compute the scaffold diversity using the information entropy. We surprisedly find out that the analogues generated by our model are not only of higher similarity with the seed molecules but also have scaffolds with higher diversity. In contrast, all baseline

models generate analogues with a lower scaffold diversity than the input drug structures.

3.3.2 SARS-CoV-2 Main Protease Inhibitor Design Case Study

Instead of de novo designing inhibitors [36], we intend to optimize existing ligand structures using our structure conditional generative model. When generating analogues of drug-like molecules, maintaining a stable 3D binding conformation is crucial for ensuring that the newly generated molecules can bind to the same protein pockets. To demonstrate that our Uni-RXN Model generates molecules that fit into the target protein pocket, we conduct a virtual screening case study. Using the 3CL_{Pro} inhibitor developed in a previous study [37] as a template, we generate a series of analogues using our model and other baseline methods. We also employ a ligand-based virtual screening protocol to retrieve candidate molecules from a large bioactive chemical library, Chember [38]. The docking results are shown in Tab. 3 and the top docking poses are shown in Fig. 5b. DINGOS (condition) is only able to generate 42 valid molecules with the template reactions while other methods do not meet this problem. The top docking scores suggest that virtual screening is not effective in finding hits for the latest protein target, even when using a chemical library of 2 million small molecules. However, our method generate molecules with higher predicted binding affinity and much more similar 3D binding conformation compared to the baseline models. These findings demonstrate that our model can aid medicinal chemists in discovering SAR in a more efficient manner by providing a large number of analogues with higher binding affinity.

Table 3 The docking scores of the generated analogues and the similarity between seed molecules and generated ones.

	DINGOS De novo (100)	DINGOS condition (42)	ChEMBL VS ¹ (100)	Uni-RXN Model (100)
Similarity _{mean} Similarity _{top} Docking Score _{mean}	0.2977	0.6548	0.4167	0.7748
	0.3816	0.7155	0.4914	0.8854
	-6.5068	-7.7953	-6.3717	-7.8301

¹VS is short for virtual screening.

The number of the generated molecules we docked with the protein pocket is listed in the (). We kept the 100 analogues that have the closest Jaccard distance to the input molecules for docking. However, the DINGOS (condition) model is only able to generate 42 valid molecules.

4 Conclusion

In this paper, we have presented a novel approach to bridging the gap between reaction-based molecule pretraining and generation tasks. Our approach has several advantages, including its ability to derive rich representations for challenging chemical reaction classification tasks. Our model outperforms other baseline models by a large margin and achieved 57.0% accuracy with only 4 data points per class provided. The transformer model can be also applied to identify errors in chemical reaction data. Without too much effort, the encoder can be applied to structure conditional generation. The experimental results have shown that the molecules our model generates are more suitable for drug discovery tasks. Our model is capable of generating molecules with more drug-like properties and synthesizable accessibility. Combined with virtual screening methods, such as molecule docking, this generative model enables efficient SAR studies. The vast synthesizable drug-like chemical space that our model generates can improve the true positive rate in drug repurposing or hit molecule searching.

5 Methods

5.1 Model Architecture

5.1.1 Pretraining Model

Transformer Model Our pretraining network applied two attentionbased models for encoders to address the multimodal nature of the chemical reaction data. The reactants and products are encoded by a graph-based transformer model, and the reagents are translated to sequence representation SELFIES [39] and then encoded by a text-based transformer model. The projection heads in contrastive learning tasks are simple MLPs with 2-layers of hidden parameters to train. We discuss the two types of transformer models we designed in the following paragraph. The text-based transformer is based on the vanilla transformer [40]. However, directly applying the transformer to reagents is non-trivial, because the tokens within chemical entities are sequential but the entities are ordering-agnostic. We develope a hierarchical transformer to model reagents. In the first step, the sequential tokens are encoded by a vanilla transformer, and the embeddings of the CLS tokens are utilized to represent the entities respectively. Then, a transformer without positional encoding is applied as the readout module from the CLS embeddings from multiple reagents.

The graph-based transformer is inspired by previous work [41]. Since molecule graphs are permutation invariant, we discard node positional encoding and applied edge encodings to embed the topological structure of the molecules. We include the bond type and an indicator token denotes whether the bond belongs to any ring as the edge feature inputs. The Atom element type, the number of formal charges, the hybridization type, and the ring indicator as in the edge feature is applied for the node feature. The edge features

are applied in our model to get the attention map as follows:

$$A_{ij} = \frac{\left(h_i W_Q\right) \left(h_j W_K\right)^T}{\sqrt{d}} + b_\phi \left(e_{ij}\right) + c_\phi SP(ij) \tag{2}$$

The h_i and h_j denote the node embeddings of node i and node j. d is the dimension of the edge features. e_{ij} is the one-hot edge feature (all zeros indicate that there are no edges between them), and SP is a function that returns the shortest path from node i to node j. b_{ϕ} and c_{ϕ} are all learnable neural networks. With this modification in attention mechanism, the model is able to capture and encode local structure while maintaining long-range interactions which are always hard to encode with message-passing neural networks. This function enables our model to learn the interaction between functional groups and understand more complicated organic chemistry. Unlike the text-based transformer model, the graph-based transformer models have a built-in readout module. The model can take multiple graphs as input, so we set the shortest path distance between atoms that do not belong to the same reactant molecules as infinity. In this way, the model automatically aggregates information within this hypergraph, where both local and global interactions are enabled.

When this graph-based transformer model is applied, we add an auxiliary node, the virtual node. It is connected to all atoms even if they belong to different molecules, the embeddings of the virtual token can be used as the results of a full graph-level readout. In the reactive center prediction task, we apply sum pooling to the embeddings from the encoder graph-based transformer and appended the CLS token from the text-based transformer as the additional input to the prediction model, which is illustrated in Fig. 2 d. This design maintains permutation invariance and allows efficient information exchange between models.

Training Objective Then we discuss the training objective of contrastive learning. In the first contrastive learning task, we want to model the interaction between reactants. Hence, the InfoNCE Loss is employed here to maximize the similarity between the embeddings of main reactants $x = c_{\text{main}}$ and their chemical reaction environment(the sub-reactants and reagents) $v = c_{\text{sub}} + c_{\text{reagent}}$. If we use X to represent all possible reactants and V to represent all possible chemical reaction environments.

$$\mathcal{L}_{InfoNCE} = -\mathbb{E}_X \left[\log \frac{f(x_i, v_i)}{\sum_{x_j \in X} f(x_j, v_i)} \right] - \mathbb{E}_V \left[\log \frac{f(x_i, v_i)}{\sum_{v_j \in V} f(x_i, v_j)} \right]$$
(3)

We apply the inner product here as the similarity function f. In the second contrastive learning task, the transformation from reactants to products is modeled by our probabilistic model. The same $\mathcal{L}_{InfoNCE}$ function is applied when $x = g_{\text{main}} + g_{\text{sub}} + g_{\text{reagent}}$ stands for chemical reaction inputs(reactants, reagents) and $v = g_{\text{product}}$ stands for chemical reaction outputs(products).

To estimate the loss efficiently, the X and V are approximated by in-batch sampled embeddings.

5.1.2 Generative Model

Conditional Variational Auto-encoder We build a conditional variational auto-encoder (CVAE) based on the pre-trained encoder to generate the representation of the responses (sub-reactants and reagents). As illustrated in Fig. 4b, we first use a long short-term memory network(LSTM) to collect the embeddings along the reaction paths we sample from the chemical reaction network [42]. Two MLP networks are designed for variational inferencing. While the recognition network takes both the target representation as inputs and the previous reaction path embeddings as inputs, the prior network only process the latter. The KL divergence between these dual latent variables is minimized like in classic variational auto-encoder models. Then the latent variable z is fed into the Top-N Set Generator to generate the target representations. During training, the prior network is trained to approximate the distribution generated from the recognition network. While generating, only the latent variable from the prior network is passed forward to the generator.

Invariant Set Generator How to generate a permutation invariant set is challenging as discussed in previous work [43]. Here we introduce a similarity-based method to generate different numbers of reactant/reagent representations from the latent variable. We store a reference parameter set, its angle is applied to decide whether we select the data points to generate representations. We denote the angle and latent variable of the reference set as Θ and R. The model is formulated as follows:

```
\begin{split} & \boldsymbol{a} = \mathrm{MLP}_1(\boldsymbol{z}) \\ & \boldsymbol{c} = \boldsymbol{\Theta} \boldsymbol{a} / \operatorname{vec} \left( \left( \left\| \boldsymbol{\theta}_i \right\|_2 \right) \right) \\ & \boldsymbol{s} = \operatorname{argsort}_{\downarrow}(\boldsymbol{c}[:n_{max}]) \\ & \tilde{\boldsymbol{c}} = \operatorname{softmax}(\boldsymbol{c}[s]) \\ & \boldsymbol{X} = \boldsymbol{R}[\boldsymbol{s}] \odot \tilde{\boldsymbol{c}} W_1 + \tilde{\boldsymbol{c}} W_2 \\ & \boldsymbol{X} = \mathrm{MLP}_2(\boldsymbol{X}, \boldsymbol{z}) \\ & \boldsymbol{Y} = \boldsymbol{X}[i_1, \cdots, i_n], \ \boldsymbol{s.t.} \ \forall i_x, \mathrm{MLP}_3(\boldsymbol{X}[i_x] > \delta) \end{split}
```

The W_1 , W_2 are trainable weight matrices, and MLP₁, MLP₂, MLP₃ are simple trainable MLP networks. n_{max} is the maximum number of responses set in the training set. θ is the threshold that we apply to decide whether to select the data points. If we use m to represent the dimension of target representations, the output \mathbf{Y} will be the $n \times m$ matrix that we need. Instead of using First-N or Top-N set generation methods, we apply a scoring network MLP₃ to determine the size of the set we generate, which helps us to generate more diverse results and update more latent variables during training.

5.1.3 Implementation of Forward Reaction Predictor

We download and deploy a server application for forward reaction prediction based on the pre-trained model from (https://github.com/pschwllr/MolecularTransformer). Though there are also other advanced models proposed recently [44], we choose this model for a fair comparison with other previously developed models. In fact, any forward reaction prediction model can be plugged into our method without much effort.

5.2 Experiment Setups

5.2.1 Negative Data Construction

To construct negative samples, we develop a workflow to sample unsuccessful chemical reactions from classified Schneider dataset [12]. Based on the fact that different classes of chemical reactions applied different sub-reactants and reagents, we apply the adding, deleting, and switching operations as the negative sample techniques. In the adding operation, random numbers of sub-reactants and reagents are sampled from reactions that belong to other reaction classes. Then they are appended to the reactions to be perturbed. While in the deleting operation, random numbers of sub-reactants and reagents are deleted. Just as the operation type implies, switching means switching random numbers of sub-reactants and reagents to chemical entities from the ones in other reaction classes. After all these processes are finished, we further filter these reactions. If the forward reaction product predictor [26] succeeds to generate a valid molecule for our perturbed reactions, it is removed from the negative sample dataset. At last, all remaining perturbed reactions are kept and form the negative data points.

5.2.2 Property Evaluation

We examine some important drug-like properties and synthetic accessibility scores to prove that our generative model is able to derive drug-like molecules based on drug structures.

Molecule weights determine the pharmacokinetics and solubility, which is really important for drug-likeness. The number of rotatable bonds describes the flexibility of 3D molecule conformations which is important when binding to the target protein. QED [45] is a popular drug-likeness quantized scoring function. LogP stands for partition coefficient which is an important physicochemical property when designing drugs. All these property scores are computed by the RDKit package.

SAScore [33], SCScore [34], and RA [35] are the synthetic accessibility scores we apply here. SAScore is a rule-based method, in which rare substructures are given a penalty for accessing the synthesizability. It also takes the topological complexity of structures into account. SCScore is a machine-learning-based score that is trained on the Reaxys database [46]. The basic hypothesis here is that the products of a reaction are always more difficult

to synthesize than the starting reactants because it requires one more step of organic reaction to derive. RAscore is another scoring function based on neural networks. There is plenty of synthetic route planning AI models developed these years, however, they are always time-consuming for larger datasets. RAscore is a classification model trained upon retrosynthetic models. It predicts the probability of a specific structure having a successful route planned by AI agents.

The validity in Tab. 2 stands for the proportion of seed molecules the model is able to generate valid analogues. The maximum depths of tree searching are set to 15 as in the original code repository for SynNet. For DINGOS (condition) model, we regard the generation process as invalid when the input seed molecules do not match with any template reactions for further modifications. In template-free models, the invalid generations represent that the predictor cannot output valid molecule smiles or one of the reactants is output as the predicted results.

In addition to validity, the distance in Tab. 2 is applied to measure the similarity between generated analogues and input seed molecules. The distance is measured by the mean Jaccard distance on the ECFP4 fingerprint of the analogues and the input seed molecules.

We also use the scaffold diversity to measure the generated molecules. Diversity is defined as the information entropy as follows:

$$H(S) = -\sum_{i=1}^{n} P(S_i) \log P(S_i)$$
 (4)

where H(S) represents the entropy of a random molecule S with possible scaffold $S_1, S_2, ..., S_n$, and $P(S_i)$ is the probability of a molecule having certain scaffold S_i . Intuitively, a high entropy indicates that the scaffolds are evenly distributed, while a low entropy indicates that there are one or a few dominant scaffolds.

5.2.3 Case Study

In the process of discovering new inhibitors for SARS-CoV-2 main protease inhibitors, we apply a workflow of virtual screening to search hit structures with high binding affinity. Firstly, the full ChEMBL database is downloaded, and the ECFP4 fingerprints are computed for all 2 million small molecule structures. We computed the Tanimoto similarity between structures from ChEMBL and the original ligand from the co-crystal structure (PDB id: 8ACL). The 100 structures with the highest similarity score are utilized as screening results. Based on the existing inhibitor, we use our model and the baseline models to generate 1000 analogues and collect the 100 structures with the highest ECFP4 similarity scores as in virtual screening.

Then we dock all generated or screened molecules to the main protease. At first, the protein structure is processed by Protein Preparation Wizard, provided by Schrodinger 2018 suite. Bond orders and missing side chains are

fixed using Prime in the preparation workflow. Waters with less than three H-bonds to amino acids are removed. The docking grid of size $10\mathring{A}\times10\mathring{A}\times10\mathring{A}$ in which the center is defined by the co-crystal ligand is saved based on the processed protein. On the other hand, the ligands' conformations and possible tautomers and protonation states are generated by the LigPrep module. The ligand conformations are docked into the pocket using Glide [47]. The default settings are applied to other parameters. The Glide docking scores are used to rank the results.

Declarations

- Data availability
 - The USTPO_MIT, USTPO_STEREO, and Schneider dataset is downloaded from the Open Reaction Database (https://docs.open-reaction-database.org/en/latest/). The reactants library we apply can be downloaded from https://zinc.docking.org/ by selecting the fragment-like subset.
- Code availability

 The pretraining and generative model in Uni-RXN are both trained on public datasets. The code are publicly available at https://github.com/qiangbo1222/Uni-RXN-official
- Competing interests

 The authors declare no competing interests.
- Authors' contributions

B.Q. conceived the initial idea for the projects. B.Q. and Y.D. processed the dataset and trained the model. B.Q. and Y.Z. performed the experiments using the pre-trained model and the generative model. Y.Z. analyzed the results and B.Q. write the manuscripts. The project was supervised by L.Z. and Z.L. All authors took part in discussions and contributed to the revising of the manuscript.

References

- [1] Devlin, J., Chang, M.-W., Lee, K., Toutanova, K.: BERT: Pre-training of Deep Bidirectional Transformers for Language Understanding. arXiv (2018). https://doi.org/10.48550/ARXIV.1810.04805
- [2] Jumper, J., Evans, R., Pritzel, A., Green, T., Figurnov, M., Ronneberger, O., Tunyasuvunakool, K., Bates, R., Žídek, A., Potapenko, A., et al.: Highly accurate protein structure prediction with alphafold. Nature 596(7873), 583–589 (2021)

- [3] Madani, A., Krause, B., Greene, E.R., Subramanian, S., Mohr, B.P., Holton, J.M., Olmos Jr, J.L., Xiong, C., Sun, Z.Z., Socher, R., et al.: Large language models generate functional protein sequences across diverse families. Nature Biotechnology, 1–8 (2023)
- [4] Jin, W., Barzilay, R., Jaakkola, T.: Junction tree variational autoencoder for molecular graph generation. In: International Conference on Machine Learning, pp. 2323–2332 (2018). PMLR
- [5] Peng, X., Luo, S., Guan, J., Xie, Q., Peng, J., Ma, J.: Pocket2mol: Efficient molecular sampling based on 3d protein pockets. In: International Conference on Machine Learning, pp. 17644–17655 (2022). PMLR
- [6] Ross, J., Belgodere, B., Chenthamarakshan, V., Padhi, I., Mroueh, Y., Das, P.: Large-Scale Chemical Language Representations Capture Molecular Structure and Properties. arXiv (2021). https://doi.org/10.48550/ ARXIV.2106.09553
- [7] Hendrycks, D., Liu, X., Wallace, E., Dziedzic, A., Krishnan, R., Song, D.: Pretrained transformers improve out-of-distribution robustness. arXiv preprint arXiv:2004.06100 (2020)
- [8] Gu, Y., Tinn, R., Cheng, H., Lucas, M., Usuyama, N., Liu, X., Naumann, T., Gao, J., Poon, H.: Domain-specific language model pretraining for biomedical natural language processing. ACM Transactions on Computing for Healthcare (HEALTH) 3(1), 1–23 (2021)
- [9] Lowe, D.M.: Extraction of chemical structures and reactions from the literature. PhD thesis, University of Cambridge (2012)
- [10] Lowe, D.: Chemical reactions from us patents (1976-sep2016). Figshare https://doi.org/10.6084/m9. figshare 5104873, 1 (2017)
- [11] Goodfellow, I., Bengio, Y., Courville, A.: Deep learning
- [12] Schneider, N., Lowe, D.M., Sayle, R.A., Landrum, G.A.: Development of a novel fingerprint for chemical reactions and its application to large-scale reaction classification and similarity. Journal of chemical information and modeling 55(1), 39–53 (2015)
- [13] Probst, D., Schwaller, P., Reymond, J.-L.: Reaction classification and yield prediction using the differential reaction fingerprint drfp. Digital discovery 1(2), 91–97 (2022)
- [14] Schwaller, P., Probst, D., Vaucher, A.C., Nair, V.H., Kreutter, D., Laino, T., Reymond, J.-L.: Mapping the space of chemical reactions using attention-based neural networks. Nature machine intelligence **3**(2),

- 144-152 (2021)
- [15] Wen, M., Blau, S.M., Xie, X., Dwaraknath, S., Persson, K.A.: Improving machine learning performance on small chemical reaction data with unsupervised contrastive pretraining. Chemical science 13(5), 1446–1458 (2022)
- [16] Wang, H., Li, W., Jin, X., Cho, K., Ji, H., Han, J., Burke, M.D.: Chemical-reaction-aware molecule representation learning. arXiv preprint arXiv:2109.09888 (2021)
- [17] Nextmove Software NameRXN. http://www.nextmovesoftware.com/namerxn.html. Accessed: 2012-11-30
- [18] Schwaller, P., Vaucher, A.C., Laino, T., Reymond, J.-L.: Prediction of chemical reaction yields using deep learning. Machine learning: science and technology **2**(1), 015016 (2021)
- [19] Chen, X., Fan, H., Girshick, R., He, K.: Improved Baselines with Momentum Contrastive Learning. arXiv (2020). https://doi.org/10. 48550/ARXIV.2003.04297
- [20] Korovina, K., Xu, S., Kandasamy, K., Neiswanger, W., Poczos, B., Schneider, J., Xing, E.: Chembo: Bayesian optimization of small organic molecules with synthesizable recommendations. In: International Conference on Artificial Intelligence and Statistics, pp. 3393–3403 (2020). PMLR
- [21] Button, A., Merk, D., Hiss, J.A., Schneider, G.: Automated de novo molecular design by hybrid machine intelligence and rule-driven chemical synthesis. Nature machine intelligence 1(7), 307–315 (2019)
- [22] Gao, W., Mercado, R., Coley, C.W.: Amortized tree generation for bottom-up synthesis planning and synthesizable molecular design. arXiv preprint arXiv:2110.06389 (2021)
- [23] Noh, J., Jeong, D.-W., Kim, K., Han, S., Lee, M., Lee, H., Jung, Y.: Path-aware and structure-preserving generation of synthetically accessible molecules. In: International Conference on Machine Learning, pp. 16952– 16968 (2022). PMLR
- [24] Coley, C.W., Barzilay, R., Jaakkola, T.S., Green, W.H., Jensen, K.F.: Prediction of organic reaction outcomes using machine learning. ACS central science 3(5), 434–443 (2017)
- [25] Jin, W., Coley, C., Barzilay, R., Jaakkola, T.: Predicting organic reaction outcomes with weisfeiler-lehman network. Advances in neural information

- processing systems 30 (2017)
- [26] Schwaller, P., Laino, T., Gaudin, T., Bolgar, P., Hunter, C.A., Bekas, C., Lee, A.A.: Molecular transformer: a model for uncertainty-calibrated chemical reaction prediction. ACS central science 5(9), 1572–1583 (2019)
- [27] Bradshaw, J., Paige, B., Kusner, M.J., Segler, M., Hernández-Lobato, J.M.: A model to search for synthesizable molecules. Advances in Neural Information Processing Systems 32 (2019)
- [28] Bradshaw, J., Paige, B., Kusner, M.J., Segler, M., Hernández-Lobato, J.M.: Barking up the right tree: an approach to search over molecule synthesis dags. Advances in neural information processing systems 33, 6852–6866 (2020)
- [29] Radford, A., Wu, J., Child, R., Luan, D., Amodei, D., Sutskever, I., et al.: Language models are unsupervised multitask learners. OpenAI blog 1(8), 9 (2019)
- [30] Irwin, J.J., Tang, K.G., Young, J., Dandarchuluun, C., Wong, B.R., Khurelbaatar, M., Moroz, Y.S., Mayfield, J., Sayle, R.A.: Zinc20—a free ultralarge-scale chemical database for ligand discovery. Journal of chemical information and modeling 60(12), 6065–6073 (2020)
- [31] Pesciullesi, G., Schwaller, P., Laino, T., Reymond, J.-L.: Transfer learning enables the molecular transformer to predict regio-and stereoselective reactions on carbohydrates. Nature communications **11**(1), 4874 (2020)
- [32] Wishart, D.S., Feunang, Y.D., Guo, A.C., Lo, E.J., Marcu, A., Grant, J.R., Sajed, T., Johnson, D., Li, C., Sayeeda, Z., et al.: Drugbank 5.0: a major update to the drugbank database for 2018. Nucleic acids research 46(D1), 1074–1082 (2018)
- [33] Ertl, P., Schuffenhauer, A.: Estimation of synthetic accessibility score of drug-like molecules based on molecular complexity and fragment contributions. Journal of cheminformatics 1, 1–11 (2009)
- [34] Coley, C.W., Rogers, L., Green, W.H., Jensen, K.F.: Scscore: synthetic complexity learned from a reaction corpus. Journal of chemical information and modeling **58**(2), 252–261 (2018)
- [35] Thakkar, A., Chadimová, V., Bjerrum, E.J., Engkvist, O., Reymond, J.-L.: Retrosynthetic accessibility score (rascore)—rapid machine learned synthesizability classification from ai driven retrosynthetic planning. Chemical Science 12(9), 3339–3349 (2021)
- [36] Morris, A., McCorkindale, W., Drayman, N., Chodera, J.D., Tay, S.,

- London, N., Consortium, C.M., et al.: Discovery of sars-cov-2 main protease inhibitors using a synthesis-directed de novo design model. Chemical Communications **57**(48), 5909–5912 (2021)
- [37] Gao, S., Sylvester, K., Song, L., Claff, T., Jing, L., Woodson, M., Weiße, R.H., Cheng, Y., Schakel, L., Petry, M., et al.: Discovery and crystallographic studies of trisubstituted piperazine derivatives as non-covalent sars-cov-2 main protease inhibitors with high target specificity and low toxicity. Journal of Medicinal Chemistry 65(19), 13343–13364 (2022)
- [38] Bento, A.P., Gaulton, A., Hersey, A., Bellis, L.J., Chambers, J., Davies, M., Krüger, F.A., Light, Y., Mak, L., McGlinchey, S., et al.: The chembl bioactivity database: an update. Nucleic acids research 42(D1), 1083–1090 (2014)
- [39] Krenn, M., Häse, F., Nigam, A., Friederich, P., Aspuru-Guzik, A.: Self-referencing embedded strings (selfies): A 100% robust molecular string representation. Machine Learning: Science and Technology 1(4), 045024 (2020)
- [40] Vaswani, A., Shazeer, N., Parmar, N., Uszkoreit, J., Jones, L., Gomez, A.N., Kaiser, L., Polosukhin, I.: Attention is all you need. Advances in neural information processing systems 30 (2017)
- [41] Ying, C., Cai, T., Luo, S., Zheng, S., Ke, G., He, D., Shen, Y., Liu, T.-Y.: Do transformers really perform badly for graph representation? Advances in Neural Information Processing Systems 34, 28877–28888 (2021)
- [42] Jacob, P.-M., Lapkin, A.: Statistics of the network of organic chemistry. Reaction Chemistry & Engineering **3**(1), 102–118 (2018)
- [43] Vignac, C., Frossard, P.: Top-n: Equivariant set and graph generation without exchangeability. arXiv preprint arXiv:2110.02096 (2021)
- [44] Chen, S., Jung, Y.: A generalized-template-based graph neural network for accurate organic reactivity prediction. Nature Machine Intelligence 4(9), 772–780 (2022)
- [45] Bickerton, G.R., Paolini, G.V., Besnard, J., Muresan, S., Hopkins, A.L.: Quantifying the chemical beauty of drugs. Nature chemistry 4(2), 90–98 (2012)
- [46] Goodman, J.: Computer software review: Reaxys. ACS Publications (2009)
- [47] Friesner, R.A., Murphy, R.B., Repasky, M.P., Frye, L.L., Greenwood, J.R., Halgren, T.A., Sanschagrin, P.C., Mainz, D.T.: Extra precision

- glide: Docking and scoring incorporating a model of hydrophobic enclosure for protein- ligand complexes. Journal of medicinal chemistry $\mathbf{49}(21)$, 6177-6196 (2006)
- [48] Johnson, J., Douze, M., Jégou, H.: Billion-scale similarity search with GPUs. IEEE Transactions on Big Data **7**(3), 535–547 (2019)
- [49] He, K., Fan, H., Wu, Y., Xie, S., Girshick, R.: Momentum contrast for unsupervised visual representation learning. In: Proceedings of the IEEE/CVF Conference on Computer Vision and Pattern Recognition, pp. 9729–9738 (2020)

Supplement A More Implementation Details

A.1 Reaction Network and Reaction Path Dataset

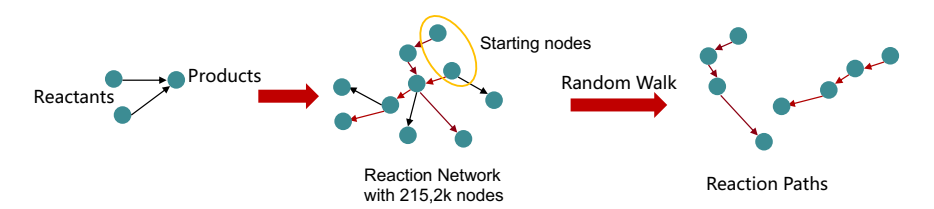


Fig. A1 An illustration of the workflow to extract reaction paths dataset to train our conditional generation model

Inspired by previous work on the reaction network [42], we first construct a chemical reaction network that consists of 2,152k nodes. Each pair of connected nodes corresponds to a chemical reaction from the USTPO STEREO dataset. The original data provides atom mapping information, so we extract the main reactants which possess the most atom mapping with the product from all reactants as the starting points of the edges. The endpoints of edges are the products of reactions. The sub-reactants and reagents are used as representations of the edges between the main reactants and products. In other words, every path in the graph represents a series of reactions that travels from one structure to another structure. All the paths derived from our reaction network are guaranteed to be valid and can be produced in wet labs.

Then, we sample paths in the graph to build our training / valid / test datasets. We select all the nodes that have a QED score higher than 0.5 to be our starting points to filter unstable reactive structures. From these nodes, we apply random walk sampling with depths from 1 to 3 in order to obtain diverse paths. Finally, we derived 970,961 valid chemical paths. The whole data processing procedure is shown in Fig .A1. The orders of the sampled paths are reversed to train the model. All the chemical paths are split as pairs of the former path and next step response (sub-reactants/ regents), so these pairs can be used for teacher force training. The inputs are the former sequences in the chemical paths, while our target is to imitate the real reactants for the coming chemical reaction editing.

A.2 Detailed Implementation of Generative Model

Our generative model is trained to approximate the representations of the target responses and predict the termination of the reaction path. Hence, there are 4 loss terms we need to minimize while training using gradient descent. The first loss term is the distance between the Set Generator generated representation of the responses with the target representation of the responses.

The inner product between representations is applied here to measure the distance. The second one is the binary cross entropy loss between the predicted selected index of X and the ground truth numbers of the responses. We also add a loss term to force the model to learn the termination of the reaction editing path, an MLP predicted whether the present responses are the last ones. Binary cross entropy is employed to train this network. The last loss term is the KL divergence between z_p and z_r as illustrated in Fig. 4b.

During inference time, our model generates complete reaction paths in the following steps. Firstly, the input molecule structure is translated to the representation using our pre-trained encoder and processed by the LSTM network. Then, the prior network outputs the z_p for the response set generation. Conditioned on the z_p , n representation is generated. We utilized the fiass package [48] developed by Facebook to search within our million-scaled precomputed reactant/ reagents representation library. The forward product predictor outputs the intermediate structure, with the generated reactants/ reagents as the input. If the network predicts it is time to terminate the generation, the product is output. Otherwise, the intermediate is appended to the reaction path for the next-step generation.

A.3 Hyperparameters

The hyperparameters of our model are chosen through a combination of manual tuning and automated searching. The hyperparameters for the model architecture are set manually. For both the graph-based transformer and text-based transformer that we employ in the shared encoders, we apply a 4-head network with a width of 512 dimensions. The transformer model we apply in the reactive center prediction task is reduced to a 2-layer model with the same number of attention heads and width dimensions. In all graph-based transformer models, we set the multi-hop edge model with a maximum distance cut-off of 6. The hidden sizes of all projection heads are 512. In the invariant generator, we set the channels of reference set to 512 and the dimension of the latent variable to 1024. The z dimension for the recognition network and prior network is set to 512. The hidden dimension of MLPs we employed in the invariant generator is also set to 512. The threshold δ for selecting data points is set to 0.5.

The batch size and learning rate are tuned by the automatic optimum finder from Pytorch Lightning. A learning rate scheduler that shrinks the learning rate to half of its value at the end of every 10 epochs is adopted too. We apply an early stopping strategy based on the loss curve of loss on the validation set.

A.4 Implementations of baselines

We evaluate our model compared to the baseline models. We include 3 methods that focused on pretraining or representation learning.

Rxnrep Inspire by contrastive learning in computer visions [49], a graph neural network model is pre-trained using a self-supervised training objective [15]. The embedding similarity between positive samples is maximized, while the ones between negative samples are minimized. The positive samples are drawn by masking atoms/ bonds/ subgraphs.

MolR Instead of contrastive learning on positive/ negative samples, MolR [16] applied training objective that maximized the embeddings between the input of the reaction (reactants/ reagents) and the output of the reaction (products). Multiple graph neural network backbones were tested in the original article. We chose the graph attention networks(GAT) backbone since it outperforms other backbones in multiple experiments.

DRFP This fingerprint is a model-free representation [13], which used a combination of two kinds of chemical fingerprints ECFP and MHFP. The circular substructures and the subsequent hashing are used to represent each molecule structure within the chemical reactions.

We include the following generative models to evaluate our generative model's performance.

SynNet A tree generation model is proposed by previous work [22]. The model is trained on artificial pathways generated from purchasable compounds and templates. We apply this model to structural analogs. However, the model is not capable to generate analogs for all drug structures. The tree-searching algorithm cannot construct any similar valid structure within the max searching depth.

DINGOS The code of DINGOS model is derived from the original article [21]. Two versions of the DINGOS model are proposed. The DINGOS (*De novo*) model chooses the starting material based on a similarity function to search for the most suitable purchasable molecule. The DINGOS (condition) takes our input drug structure as the starting material and generates one step of reaction modification based on the neural network predicted template reaction and building blocks. The product of the template reaction is collected as the structure analog.

MolChef We download the code of [27] from the Github repository and deploy the model with its original setting. This model generates molecules unconditionally by sampling building blocks and generates the reaction product using the same product prediction model [26] as in our works. We include this model to prove that the template-free model generates more synthesizable molecules

Supplement B Additional Experiments

B.1 TPL 1k Classification Task

Following previous work [14], we test our model on the TPL 1k reaction classification dataset. This is a rule-based classification system and the benchmark dataset is unbalanced. In addition to accuracy, we also evaluate the confusion

entropy of the CEN metric which provide a fair comparison of multi-class classification tasks. When we denote Matrix as the confusion matrix, the CEN can be derived as follows:

$$\begin{split} P_{i,j}^j &= \frac{\operatorname{Matrix}(i,j)}{\sum_{k=1}^{\mathsf{C}} (\operatorname{Matrix}\ (j,k) + \operatorname{Matrix}(k,j))} \\ P_{i,j}^i &= \frac{\operatorname{Matrix}(i,j)}{\sum_{k=1}^{\mathsf{C}} (\operatorname{Matrix}\ (i,k) + \operatorname{Matrix}(k,i))} \\ \operatorname{CEN}_j &= -\sum_{k=1,k\neq j}^{\mathsf{C}} \left(P_{j,k}^j \log_{2(\mathsf{C}-1)} \left(P_{j,k}^j \right) + P_{k,j}^j \log_{2(\mathsf{C}-1)} \left(P_{k,j}^j \right) \right) \\ P_j &= \frac{\sum_{k=1}^{\mathsf{C}} (\operatorname{Matrix}(j,k) + \operatorname{Matrix}(k,j))}{2\sum_{k,l=1}^{\mathsf{C}} \operatorname{Matrix}(k,l)} \\ \operatorname{CEN} &= \sum_{j=1}^{\mathsf{C}} P_j \operatorname{CEN}_j \end{split}$$

The results are shown in Table. B1. Our model shows comparable accuracy with other methods and outperforms other baseline methods on the CEN metrics. These results illustrate that our model not only performs well on small datasets but also is able to provide comparable performance on large datasets. rxnfp[14] outperforms our model by 6.2%, when pretraining on a commercial dataset that possesses 2 million hand-curated data instead of an openly accessible database that possesses 500k noisy data. DRFP outperforms our model by using a rule-based fingerprint, which takes short-cut when benchmarking on a rule-based classification task.

Methods	Accuracy	CEN
AP3 256 (MLP)	0.809	0.101
AP3 256 (5-NN)	0.295	0.242
DRFP $(5-NN)$	0.917	0.041
DRFP (MLP)	0.977	0.011
rxnfp	0.989	0.006
hypergraph	0.928	_1
Uni-RXN	0.927	0.003

¹The CEN results are missing because the original paper does not provide the code to reproduce the predictions.

B.2 Ablation Study

In order to verify the function of our pre-trained encoder in the generative model, we carry out an ablation study to prove that these pretraining tasks aid our generative model to generate sub-reactants and reagents accurately. We remove the shared encoder in different stages and replaced it with encoders that are trained from scratch or other fingerprints encoding. Because different representation is used to encode the target structure, it is not suitable to measure the quality using representation distances. Therefore, we randomly select a batch of other reactants/ reagents with different representations encoded and rank the ground truth target representation among this batch of representations. A Low ranking number indicates that our model generates representations that are more likely to retrieve the plausible reactants/ reagents from the library. The results are listed in Table, B2.

 ${\bf Table~B2~~Ablation~study~results~of~the~model~with~different~encodings~of~target~and~input~structures}$

Uni-RXN Input	Uni-RXN Target	Pretrained Encoder	Ranking scores
-	-	-	0.3474
√	-	-	0.2451
-	✓	✓	0.2304
√	✓	-	0.3486
√	✓	✓	0.1243

The lower ranking scores indicate better performance. We used ECFP4 as the encodings for molecule structures if we remove the pre-trained encoders.

The results illustrate that without the pre-trained encoder, the generative model is not able to approximate the data distribution of the corresponding sub-reactants/ reagents. When we use ECFP4 as the fingerprints to encode our molecule structure, our model's ranking scores increase which means the fingerprint-based model fail to differentiate molecules that play different roles in chemical reactions. However, this encoding strategy is applied in a few related works [21, 22]. In conclusion, the ablation study shows that our Uni-RXN embedding is a good representation of chemical entities in the reactions. The trained encoders help our model generates responses that maintain the consistency of the input structures.

B.3 Yield Regression Experiment

First, we design a weighted K-Neighbor method to predict the yield of the chemical reactions. It is hard to predict the chemical reaction yields for the

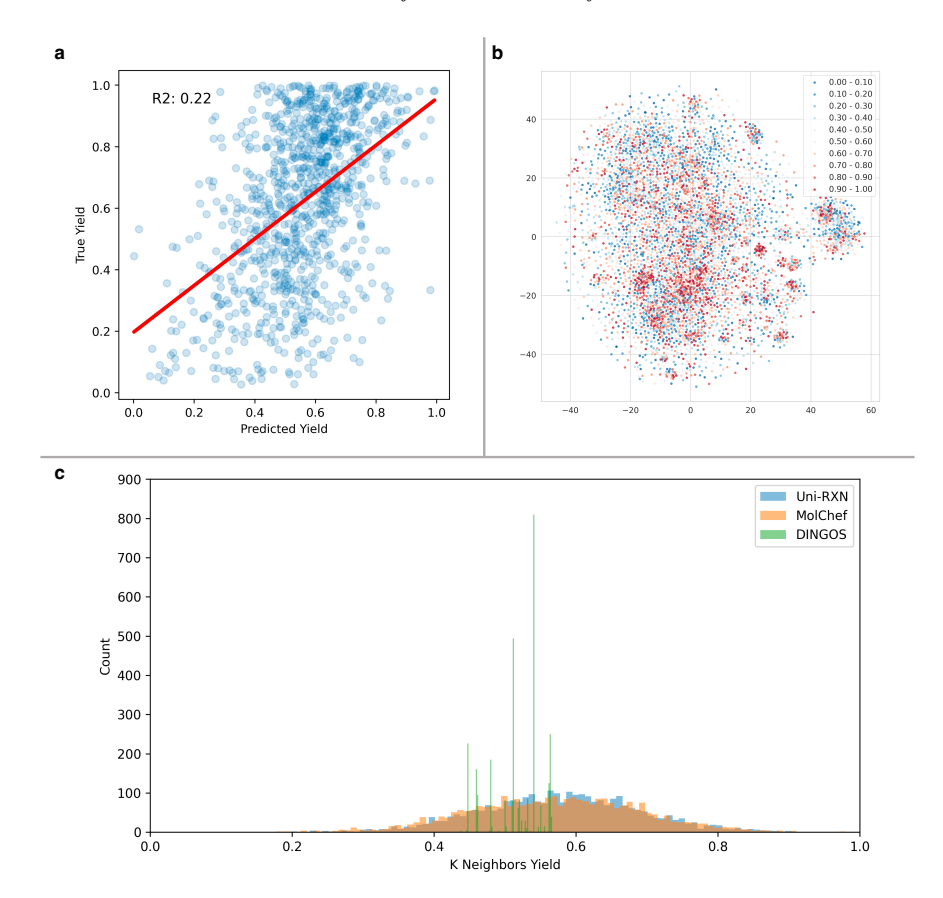


Fig. B2 (a) The relation between our model predicted K-Neighbor yield and ground truth yield. (b) The T-SNE visualization of the Uni-RXN chemical reaction space colored with yield data. (c) The distribution of the chemical reactions' predicted yields proposed by different methods.

open patent dataset because the dataset is noisy and has an unsmooth yield landscape [18]. We use a weighted K-neighbor method to predict the yield. Specifically, we search for the K nearest neighbors in the chemical reaction space encoded by Uni-RXN encoders. If we denote the K nearest distances as D and the yield of these K reactions as L. The predicted yield y can be derived as:

$$y = \frac{\sum_{i \in 1 \dots K} (1/D_i * L_i)}{\sum_{i \in 1 \dots K} (1/D_i)}$$
(B1)

When we exclude 1000 data from the USTPO dataset to test our method's ability. The result is illustrated in Fig. B2(a). In the only previous work [18] that tested its performance to predict yield on the USTPO dataset, they achieve results of R_2 less than 0.2 on the gram and sub-gram dataset. Our model clearly outperforms their methods by a large margin and is suitable to predict the approximation of the reaction yield. The visualization results in

Fig. B2(b) demonstrates that though the landscape is still unsmooth, the well-optimized reactions with high yield ranging from 90% 100% are clearly well clustered in our chemical reaction space.

Based on this K-neighbor method, we predict the yield for the reactions generated by the template-based method and the template-free method. The results are plotted in Fig. B2(c). We can see that the template reactions with the green color in Fig. B2(c) are not well-optimized. However, the template-free methods (Uni-RXN, MolChef) generate more high-yield reactions. The average predicted yield for the reactions generated by our model is 57.68%. For MolChef model [27], the predicted yield is 57.02%. Our method outperforms both another template-free model and the template-based method.